

Deciphering the quenching mechanism of 2D MnO₂ nanosheet towards Au nanocluster fluorescence to design effective glutathione biosensor

Shichao Lin,^{†‡} Hanjun Cheng,^{†§§} Qiran Ouyang,[†] and Hui Wei^{*†}

[†]Department of Biomedical Engineering, College of Engineering and Applied Sciences, Collaborative Innovation Center of Chemistry for Life Sciences, Nanjing National Laboratory of Microstructures, Nanjing University, Nanjing 210093, China.

[§]State Key Laboratory of Analytical Chemistry for Life Science, Nanjing University, Nanjing 210093, China.

Characterization of 2D MnO₂ nanosheets

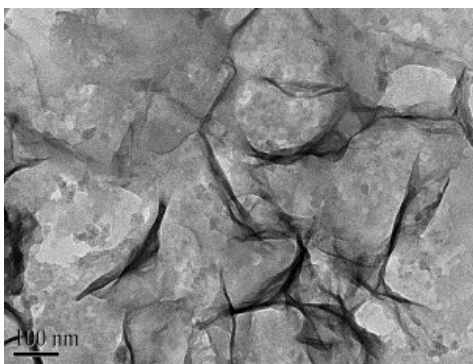


Figure S1. Typical TEM image of as-prepared ultrathin MnO₂ nanosheets.

Contribution of FRET to the Fluorescence Quenching

The fluorescence quenching efficiency contributed from fluorescence resonance energy transfer (FRET) was calculated according to the following equations in assumption that the donor (i.e. AuNC@BSA) and the acceptor (i.e., MnO₂ nanosheets) were randomly distributed in 3D solutions.¹

$$E = 1 - \frac{F_{DA}}{F_D} \quad 1.$$

$$\frac{F_{DA}}{F_D} = 1 - \gamma \sqrt{\pi} \exp(-\gamma^2) [1 - \operatorname{erf}(\gamma)] \quad 2.$$

$$\operatorname{erf}(\gamma) = \frac{2}{\sqrt{\pi}} \int_0^\gamma \exp(-x^2) dx \quad 3.$$

$$\gamma = A/A_0 \quad 4.$$

$$A_0 = \frac{3000}{2\pi^{3/2}NR_0^3} \quad 5.$$

$$R_0 = 0.211(k^2n^{-4}\varphi_DJ(\lambda))^{1/6} \quad (\text{in } \text{\AA}) \quad 6.$$

$$J(\lambda) = \frac{\int_0^\infty F(\lambda)\varepsilon(\lambda)\lambda^4 d\lambda}{\int_0^\infty F(\lambda)d\lambda} \quad 7.$$

Where, $F(\lambda)$ is the fluorescence intensity of AuNC@BSA at the wavelength of λ , and $\varepsilon(\lambda)$ is the corresponding molar extinction coefficient of MnO₂ nanosheets at that λ .¹ The overlap integral $J(\lambda)$ indicates the degree of overlap between the donor emission spectrum and the acceptor absorption spectrum.¹ k^2 is the orientation factor describing the dipole-dipole interaction between donor and acceptor (here, $k^2=2/3$).^{1,2} n is the refractive index of the medium (here, $n=1.45$). R_0 is the Förster distance of the paired donor and acceptor, which is the critical distance at which the energy transfer efficiency is 50%. φ_D is the fluorescence quantum yield of the donor in the absence of acceptor (here, $\varphi_D=0.06$). N is Avogadro's number. A_0 is the critical concentration, representing the acceptor concentration A that results in 76% energy transfer.¹ The calculated $J(\lambda)$, R_0 , and A_0 were listed in Table S1. The fluorescence quenching efficiency (E) contributed by FRET at different concentrations of MnO₂ nanosheets was then calculated with Equation 1.

Table S1. Parameters used to estimate the FRET between AuNC@BSA and MnO₂ nanosheets.

	$J(\lambda)$	R_0 (nm)	A_0 (mM)
AuNC@BSA	2.75×10^{14}	2.46	30

Contribution of IFE to the Fluorescence Quenching

The fluorescence quenching efficiency contributed from inner filter effect (IFE) was calculated according to the following equations.^{1,3}

$$E = 1 - \frac{F}{F_0} \quad 8.$$

$$\frac{F_{cor}}{F_{obsd}} = \frac{2.3dA_{ex}}{1 - 10^{-dA_{ex}}} 10^{gA_{em}} \frac{2.3sA_{em}}{1 - 10^{-sA_{em}}} \quad 9.$$

Where, F and F_0 are the fluorescence intensities of AuNC@BSA in the presence and absence of MnO₂ nanosheets, respectively. F_{obsd} is the observed fluorescence intensity and F_{cor} is the corrected fluorescence intensity by removing IFE contribution from F_{obsd} . A_{ex} and A_{em} represent the absorbance at the excitation wavelength ($\lambda_{ex}=365$ nm) and emission wavelength ($\lambda_{em}=653$ nm), respectively.^{1,2} d is the width of the cuvette (2 mm), g is the distance between the edge of the excitation beam and the edge of the cuvette (4 mm) and s is the width of the excitation beam (1 mm) (Figure S2).

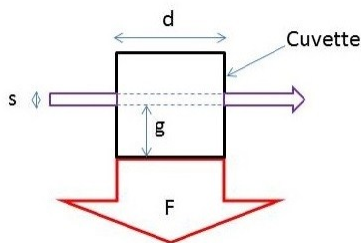


Figure S2. Cuvette geometry and parameters used in Equation 9.

Table S2. Parameters used to estimate the FRET between AuNC@BSA and MnO₂ nanosheets.

MnO ₂ (μM)	A_{ex}	A_{em}	F_{obsd}	F_{cor}	CF	F_{cor0}/F_{cor}
0	0.086	0.005	519.8	530.2	1.02	1.00
100	0.189	0.028	372.0	398.0	1.07	1.33
200	0.295	0.052	221.7	250.5	1.13	2.12
300	0.402	0.076	128.7	151.9	1.18	3.49
400	0.501	0.098	82.8	102.7	1.24	5.16
500	0.614	0.122	52.1	65.1	1.25	8.14
600	0.719	0.144	39.7	54.0	1.36	9.83

Table S2 summarizes the parameters used in calculating the contribution of IFE to the fluorescence quenching process. Corrected factor (CF) was defined as $CF = F_{cor}/F_{obsd}$. The maximum of CF should not exceed 3, otherwise the value of the correction is not convincing. F_{cor0} and F_{cor} are the corrected fluorescence intensity of AuNC@BSA in the absence and presence of MnO₂ nanosheets.^{1,2}

Contribution of DQE and SQE to the Fluorescence Quenching

The fluorescence quenching efficiency contributed from dynamic quenching effect (DQE) and static quenching effect (SQE) was calculated according to the following Equation 10 (Figure S3).¹

$$\frac{F_0}{F} = 1 + K_{SV}[Q] \quad 10.$$

Where, F_0 and F are the steady state fluorescence intensities in the absence and presence of the quencher (i.e., MnO₂ nanosheets), respectively. $[Q]$ is the concentration of MnO₂ nanosheets.

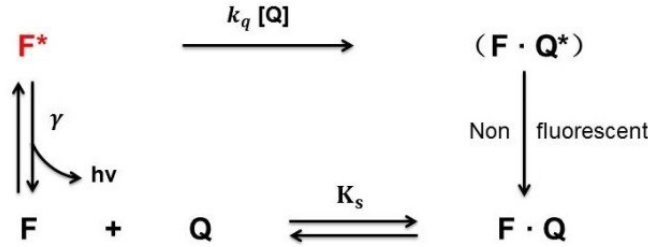


Figure S3. Illustration of dynamic quenching process and static quenching process.¹

For DQE, it follows the Stern-Volmer equation below:

$$\frac{F_0}{F} = 1 + k_q \tau_0 [Q] = 1 + K_D [Q] \quad 11.$$

Where, k_q is the bimolecular quenching constant; τ_0 is the lifetime of the fluorophore in the absence of quencher.

For SQE, it follows the Stern-Volmer equation below:

$$\frac{F_0}{F} = 1 + K_S [Q] \quad 12.$$

For both DQE and SQE involved with the same fluorophore, it follows the Stern-Volmer equation below:

$$\frac{F}{F_0} = \frac{1}{1 + K_S [Q]} \cdot \frac{1}{1 + k_q \tau_0 [Q]} \quad 13.$$

Equation 13 can be rearranged into the following form by inversion:

$$\frac{F_0}{F} = K_D K_S [Q]^2 + (K_D + K_S) [Q] + 1 \quad 14.$$

This modified form of the Stern-Volmer equation is second order in $[Q]$, which assumes that both the dynamic and static quenching processes are involved with the same fluorophore (here MnO_2 nanosheets). By fitting the data, $K_D K_S = 3.59 \times 10^{-5} (\mu\text{M})^{-2}$ and $K_D + K_S = 3.07 \times 10^{-4} (\mu\text{M})^{-1}$ could be obtained.

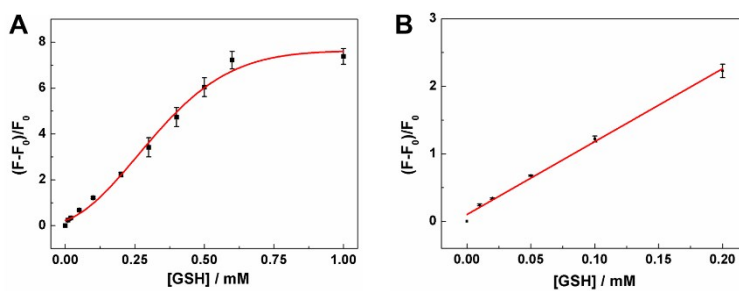


Figure S4. Detection of GSH using 400 μM MnO_2 nanosheets. (A) Plot of $(F-F_0)/F_0$ versus GSH concentration. (B) Linear response of $(F-F_0)/F_0$ to GSH concentration. Error bars indicate standard deviations of three independent measurements.

When 400 μM MnO_2 nanosheets were used for GSH detection, a detection limit of 4 μM towards GSH was obtained. This indicated that the sensing performance of the current method could be tuned by changing the concentration of MnO_2 nanosheets.

Table S3. Comparison of the proposed approach with other reported methods for the detection of GSH.

Methods	Linear range (μM)	LOD (μM)	Reference
Fluorimetry	0.1-20	0.03	4
Fluorimetry	N/A	0.9	5
Fluorimetry	0-100	0.2	6
Fluorimetry	0-600	0.022	7
Fluorimetry	0-100	0.83	8
Fluorimetry	1-10	0.8	9
Fluorimetry	0-500	4	This work

References

- (1) Lakowicz, J. R. *Principles of Fluorescence Spectroscopy*, Springer: **2006**.
- (2) Zhai, W. Y.; Wang, C. X.; Yu, P.; Wang, Y. X.; Mao, L. Q. *Anal. Chem.* **2014**, *86*, 12206-12213.
- (3) Gauthier, T. D.; Shane, E. C.; Guerin, W. F.; Seitz, W. R.; Grant, C. L. *Environ. Sci. Technol.* **1986**, *20*, 1162-1166.
- (4) Jiang, X. Y.; Geng, F. H.; Wang, Y. X.; Liu, J. H.; Qu, P.; Xu, M. T. *Biosens. Bioelectron.* **2016**, *81*, 268-273.
- (5) Deng, R. R.; Xie, X. J.; Vendrell, M.; Chang, Y. T.; Liu, X. G. *J. Am. Chem. Soc.* **2011**, *133*, 20168-20171.
- (6) Meng, H. M.; Jin, Z.; Lv, Y. F.; Yang, C.; Zhang, X. B.; Tan, W. H.; Yu, R. Q. *Anal. Chem.* **2014**, *86*, 12321-12326.
- (7) Wang, Y. H.; Jiang, K.; Zhu, J. L.; Zhang, L.; Lin, H. W. *Chem. Commun.* **2015**, *51*, 12748-12751.
- (8) Li, N.; Diao, W.; Han, Y. Y.; Pan, W.; Zhang, T. T.; Tang, B. *Chem. Eur. J.*, **2014**, *20*, 16488-16491.
- (9) Tang, Q.; Wang, N. N.; Zhou, F. L.; Deng, T.; Zhang, S. B.; Li, J. S.; Yang, R. H.; Zhong, W. W.; Tan, W. H. *Chem. Commun.*, **2015**, *51*, 16810-16812.